MALAYSIAN JOURNAL OF ANALYTICAL SCIENCES

Journal homepage: https://mjas.analis.com.my/

Research Article

Integrated structural, thermal, and electrochemical analysis of gold-modified activated carbon–polyurethane electrodes

Muhammad Abdurrahman Munir[1*], Fitria Rahmawati[2], David Fernando[3], Imam Shofid Alaih[2], Ahlam Inayatullah[4], and Abdul Rohman[2]

[1]Faculty of Resource Science and Technology, Universiti Malaysia Sarawak, 94300, Kota Samarahan, Malaysia
[2]Research Group of Solid Chemistry and Catalysis, Chemistry Department, Faculty of Mathematics and Natural Sciences, Sebelas Maret University, 57126, Surakarta, Indonesia
[3]Department of Pharmaceutical Chemistry, Faculty of Pharmacy, Universitas Gadjah Mada, Yogyakarta 55281, Indonesia
[4]Food Technology Study Program, Chemical Engineering Department, Sriwijaya State Polytechnic, 30128, Palembang, Indonesia

[*]Corresponding author: mmabdurrahman@unimas.my

Received: 25 September 2025; Revised: 16 December 2025; Accepted: 5 January 2026; Published: 28 February 2026

Abstract
This study presents the development and comprehensive characterization of bio-based polyurethane (PU) composites reinforced with gold (Au) nanoparticles for multifunctional performance enhancement. The PU matrix was synthesized using methylene diphenyl diisocyanate (MDI) and palm kernel oil-derived polyol, while Au nanoparticles were incorporated at varying loadings (1, 2, 5, and 10 wt%) via a sonication-assisted solution casting technique. Fourier Transform Infrared Spectroscopy (FTIR) confirmed the structural integrity of the PU backbone and suggested non-covalent interactions, such as hydrogen bonding, between Au and polar groups in the matrix. Principal Component Analysis (PCA) of FTIR data further distinguished composite formulations based on spectral variations, highlighting the influence of Au at the molecular level. Field Emission Scanning Electron Microscopy (FESEM) revealed uniform dispersion of Au with minimal aggregation, supporting strong matrix-filler interaction. Thermogravimetric Analysis (TGA) and Differential Scanning Calorimetry (DSC) showed satisfactory thermal stability, delayed degradation, and increased char residue, especially at 5–10 wt% Au, attributed to Au's high thermal conductivity and barrier effect. Electrochemical Impedance Spectroscopy (EIS) revealed that increasing the Au content reduces the resistance value, suggesting the creation of efficient conductive pathways.

Keywords: activated carbon, gold nanoparticles, nanocomposites, polyurethane composites

Introduction

Producing a sophisticated functional material by adding conductive fillers has a high demand, particularly for electrochemical and environmental applications. Polyurethane (PU)-based composites have attracted many researchers owing to their flexibility to include a wide range of additives, chemical durability, and adjustable mechanical strength [1]. Activated carbon (AC), known for its high porosity, wide surface area, and satisfactory electrical conductivity, is commonly used to improve the performance of PU [2]. Gold (Au) is one of the nanoparticles that is generally applied on the surface of activated carbon to improve the AC performance, including thermal stability, catalytic activity, and more efficient electron transport. Several studies reported that the gold-modified activated carbon/polyurethane composites (Au-AC/PU) are gaining attention as adaptable possibilities for next-generation electrode materials [3].

Despite this growing interest, current research on PU-based conductive composites presents several unresolved limitations. Most existing studies focus on conventional structural, thermal, and electrochemical characterization, yet they fall short in capturing overlapping FTIR features, subtle thermal transitions, and complex degradation mechanisms. Additionally, while gold-modified activated carbon has shown potential advantages, the literature lacks a systematic understanding of how the Au-modified filler influences molecular interactions, structural

modifications, and performance enhancement within PU matrices. The absence of deeper analytical treatment limits the clarity of structure–property relationships, indicating a clear research gap in establishing a comprehensive and detailed evaluation of the functional role of Au within PU composites [3,4].

Numerous researchers have reported the properties of composite materials, with a focus on thermal stability, chemical structure modification, morphology, and electrochemical performance, and many of researchers used common instruments, including the FTIR, thermogravimery analysis (TGA), scanning electron microscopy (SEM), differential scanning calorimetry (DSC), and electrochemical impedance spectroscopy (EIS), nevertheless, they often lack the statistical depth needed to resolve overlapping peaks or complex thermal transitions [4-6]. Techniques such as FTIR, and TGA, without coupling with the chemometric approach, provide highly multivariate results that might be difficult to comprehend qualitatively, limiting a thorough knowledge of material behavior [7]. Furthermore, chemometric methods are available for detecting patterns and trends in large datasets; their application in characterizing AC-based polymer composites is considerable [8], yet is still uncommon. Methods including the Partial Least Squares Regression (PLSR) and Principal Component Analysis (PCA) have proven to be effective in other areas of materials study, where they improve in data reduction, signal clarity, and reliable quantitative validation. Nevertheless, their application in comprehending and identifying the FTIR and TGA data in investigations on gold-modified polymer/carbon composites is particularly underexplored [9,10].

This study presents an approach to determine gold-modified activated carbon-polyurethane (Au-AC/PU) composites using a chemometric approach coupled with FTIR and TGA. By using statistical approaches, it delivers deeper insights into the materials' thermal and structural properties, allowing for the interpretation of complicated spectral and thermal patterns that standard approaches may miss. Chemometric modeling improves our comprehension of functional group interactions and decomposition mechanisms. Overall, this data-driven approach goes beyond traditional characterization to provide a more comprehensive and dependable framework for analyzing and optimizing composite electrodes in advanced functional material applications.

Materials and Methods

Materials

Polyurethane (PU) was produced using the Munir et al. method [11], with a few modifications. The 4,4-diphenylmethane diisocyanate (MDI) and the palm kernel oil (PKO) were purchased from PT Chemie Mitra Indonesia. Gold (Au) and N, N-dimethylformamide (DMF) were purchased from Sigma Aldrich, Indonesia. All chemicals used in the studies were analytical grade to ensure precision and dependability. To ensure uniformity and minimize deterioration throughout processes, all solution preparations were made using deionized water kept at 4 ℃.

Fabrication of PU/Au

The fabrication of PU/Au composites followed the method reported by Naseem et al. (2024), with minor modifications [12]. Gold (Au) with various concentrations, such as 1, 2, 5, and 10 wt%, was prepared by dissolving the corresponding amounts in dimethylformamide (DMF) within an Erlenmeyer flask. To promote thorough dispersion, the solutions were sonicated at 60 ℃ Under continuous magnetic stirring. Water was added during sonication to stabilize the temperature. The process was continued until a dark, ink-like appearance was observed, indicating effective dispersion of the gold. Next, approximately 5 mL of polyurethane (PU) solution was introduced into each gold dispersion, and stirring was continued until a uniform blend was achieved. The resulting mixtures were cast into molds and subjected to solvent evaporation in a vacuum oven at 60 ℃ for 6 hours, yielding homogeneously integrated PU/Au composite films.

Comprehensive characterization of PU/Au composites: PCA-Assisted FTIR and TGA analysis with FESEM, DSC, and EIS evaluation

Before analysis, PU/Au films were equilibrated at ambient conditions for 24 hours. *Surface Morphology*: The surface features of the PU/Au composites were examined using a Field-Emission Scanning Electron Microscope (FESEM, model JSM-6510 LA), coupled with Energy Dispersive X-ray (EDX) spectroscopy to determine elemental composition and confirm gold dispersion. *Thermal Characterization*: *Thermogravimetric Analysis (TGA)*: Thermal stability assessments were conducted using a PerkinElmer Pyris TGA system. Approximately 10 mg of each sample was sectioned and analyzed from 40 ℃ to 800 ℃ at a heating rate of 25 ℃•min^{-1} under a constant nitrogen flow of 50 mL•min^{-1}. Derivative thermogravimetry (DTG) data were subjected to Principal Component Analysis (PCA) to distinguish thermal degradation profiles among PU, PU/Au, and pure Au. PCA was performed using *Orange Software version 3.36.1* [13]. *Differential Scanning Calorimetry (DSC)*: The thermal transitions of PU/Au composites were studied using a PerkinElmer Pyris DSC. Samples (~10 mg) were hermetically sealed in

aluminum pans and heated from 25 ℃ to 150 ℃ at 20 ℃•min^{-1}, held isothermally for 3 minutes, then rapidly cooled to –100 ℃. A second heating cycle was conducted from –100 ℃ to 200 ℃. The glass transition temperature (*Tg*) was determined from the inflection point of the heat flow curve. *Chemical Characterization*: *FTIR Analysis*: Fourier Transform Infrared (FTIR) spectroscopy was used to investigate chemical bonding within the PU/Au composites. Spectra were collected using a Thermo Scientific Nicolet iS10 system with a Diamond Attenuated Total Reflectance (DATR) accessory. Key functional groups, including –NH, –CH, –NCO, and –C=O, were analyzed to verify the composite structure. PCA was applied to absorbance data to assess differences among PU/Au, neat PU, and MDI, with heatmaps visualized using *MetaboAnalyst version 6.0.0* [14,15]. *Electrical Conductivity*: *Electrochemical Impedance Spectroscopy (EIS)*: The electrical characteristics of PU/Au composites were evaluated via Electrochemical Impedance Spectroscopy using an Electrochemical Workstation at Sebelas Maret University. The electrochemical measurements were carried out using a three-electrode setup, where PU/Au served as the working electrode, a platinum wire was used as the counter electrode, and Ag/AgCl acted as the reference electrode. All experiments were performed at room temperature under open-circuit potential (OCP), covering a frequency range from 10 kHz to 10 MHz with a 10 mV signal amplitude. The collected impedance spectra were then processed using ZView software to evaluate the resistance and capacitance characteristics.

Results and Discussion

The FTIR was used to examine the chemical structure of the synthesized PU and the PU/Au composites, as illustrated in **Figure 1**. At the same time, **Table 1** lists the sixteen selected absorption wavenumbers used for PCA analysis. The purpose of this analysis was to verify the successful formation of the polymer and to investigate how the gold particles interact with the polyurethane matrix. Key functional groups associated with the PU backbone were identified to evaluate molecular compatibility, filler distribution, and possible interaction mechanisms within the composite. These spectral features act as important markers for understanding polymer crosslinking and phase behavior [16,17].

The presence of urethane amide linkages is found in the ~3200 cm^{-1}, indicating the reaction between the hydroxyl-containing polyols and isocyanate groups in MDI. Aliphatic C-H stretching at ~2900 cm^{-1} can be found in PKO and polyethylene glycol. Furthermore, the absence of a peak around ~2270-2400 cm^{-1} in PU, where these wavenumbers are attributed to the isocyanate (-N=C=O) group, indicates that the isocyanates were completely consumed during polymerization. Liu & Ma and Hennig et al. found that a well-crosslinked PU matrix was successfully formed with few unaffected species [18,19]. Additional absorption bands observed near ~1300 cm^{-1} correspond to carbamate (C–NH) bonds, while those around ~1100 cm^{-1} indicate the presence of C–O–C ether linkages in the polyether soft segments. These spectral features align well with the expected chemical structure of polyurethane derived from methylene diphenyl diisocyanate (MDI) and palm kernel oil-based polyester polyol. The absence of absorption near ~1690 cm^{-1}, where urea C=O stretching normally appears, suggests that side reactions between isocyanates and moisture, commonly leading to urea formation, were effectively minimized under controlled synthesis conditions [20,21].

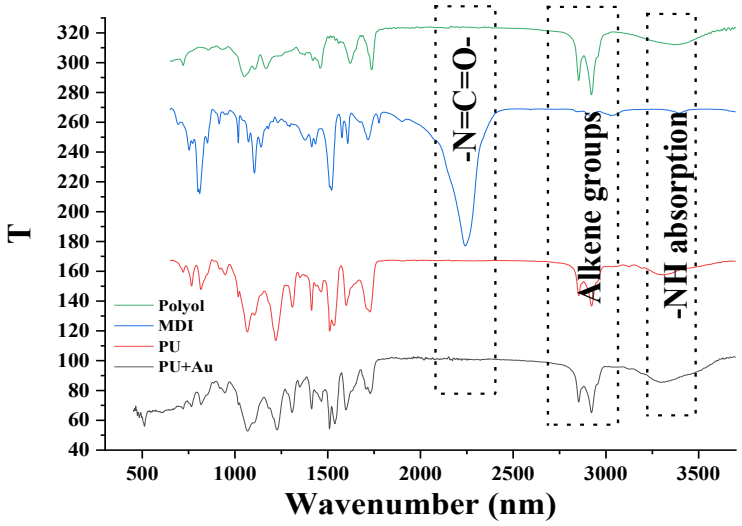

Figure 1. FTIR spectral profile of PU/Au (10%), PU, MDI, and Polyol

Table 1. Analysis of Infrared Spectral Characteristics of PU/Au, PU, MDI, and Polyol

No.	Peak Wavenumber (cm^{-1})	Functional Group Interpretation	Vibration Mode	Intensity	Wavenumber Range Reference (cm^{-1})	Dominant Compound
1	3338	N–H (urethane or amine) or O–H (polyol)	Stretching	Broad, Strong	3700-3200	PU, PU/Au, Polyol
2	2922	Aliphatic alkane (C-H)	Stretching	Strong	3000-2850	PU, PU/Au, Polyol
3	2853	Aliphatic alkane (C-H)	Stretching	Strong	3000-2850	PU, PU/Au, Polyol
4	2241	Isocyanate (-N=C=O)	Asymmetric stretching	Strong	2276-2240	MDI
5	1729	C=O in urethane (-COO)	Stretching	Strong	1750-1730	PU, PU/Au, Polyol
6	1599	Aromatic C=C	Stretching	Medium-weak	1600-1475	PU, PU/Au
7	1539	Amide N-H (-NHCOO- in urethane linkage)	Bending	Medium-Strong	1640-1550	PU, PU/Au
8	1466	Alkane C-H	Bending	Medium	1450-1375	PU, PU/Au, Polyol
9	1413	CH_2 scissoring or O–H bending	Scissoring or bending	Medium	144-1380	PU, PU/Au, MDI
10	1350	Amine C-N	Stretching	Medium-strong	1350-1000	PU, PU/Au
11	1308	C-O (Ester) in urethane linkage	Stretching	Strong	1300-1000	PU, PU/Au
12	1228	C-O (Ester) in urethane linkage	Stretching	Strong	1300-1000	PU, PU/Au
13	1068	C-O (Ester) in urethane linkage	Stretching	Strong	1300-1000	PU, PU/Au, Polyol
14	946	Aromatic C-H	Out-of-plane bending	Strong	1000-650	PU/Au, PU (weaker)
15	817	Aromatic C-H	Out-of-plane bending	Strong	1000-650	PU/Au, PU (weaker), MDI
16	758	Aromatic C-H	Out-of-plane bending	Strong	1000-650	PU/Au, PU (weaker), MDI

Although gold (Au) lacks IR-active vibrational modes due to its metallic nature, its presence can be inferred from subtle changes in the polymer's FTIR spectrum [22]. No distinct Au absorption bands were observed, but shifts in –C=O (~1700 cm^{-1}) and –N–H peaks suggest non-covalent interactions, such as electron donation or coordination with PU groups. Broadened O–H/N–H peaks indicate possible hydrogen bonding near Au particles [23]. Sixteen wavenumber absorptions were chosen for PCA based on their correlation to functionally and structurally important vibrations within the MDI, polyol, PU, and PU/Au systems (**Table 1**). These peaks signify essential chemical transformations, such as urethane linkage formation, hydrogen bonding interactions, and aromatic segment behavior. Their incorporation facilitates targeted multivariate analysis centered on the most diagnostically significant features, minimizing interference from extraneous or overlapping spectrum regions.

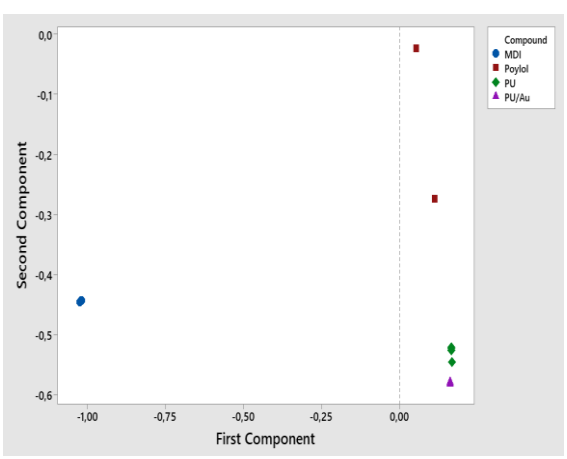

(a)

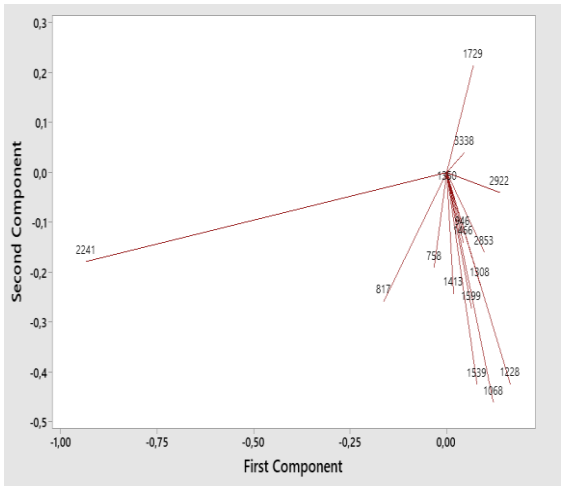

(b)

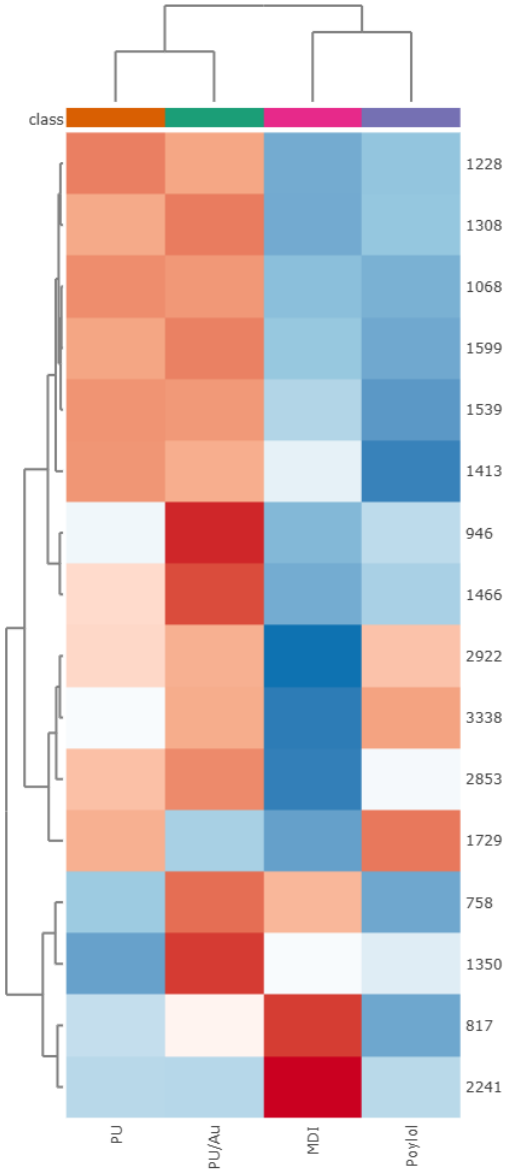

(c)

Figure 2. Principal Component Analysis (PCA) of FTIR spectra of MDI, PU, PU/Au, and Polyol based on absorption at 16 selected wavenumbers: (a) Score plot showing sample distribution along PC1 and PC2, (b) Loading plot illustrating the contribution of each wavenumber to the principal components, and (c) Heatmap visualization (Euclidean distance) of MDI, PU, PU/Au, and Polyol

Silipigni et al. found that incorporating AuNPs into PLA films increased IR absorption intensity without shifting characteristic peaks, suggesting good dispersion and no new chemical bonding [22]. Conversely, Martis et al. observed OH peak shifts and a reduction in intensity in PVA systems, indicating coordination between AuNPs and hydroxyl groups [24]. FTIR spectroscopy, combined with Principal Component Analysis (PCA), effectively differentiates between PU, PU/Au, MDI, and polyol materials (**Figure 2a**). PCA revealed that PC1, explaining most spectral variation, is dominated by the 2241 cm^{-1} isocyanate (–N=C=O) band with a strong loading of –0.935 (**Figure 2b**). PC2, influenced by the 1068 cm^{-1} band (loading –0.461), further separates PU, PU/Au, and polyol. PC1 alone distinguishes MDI, while PC1 and PC2 together account for 97.3% of the variation, highlighting the critical role of isocyanate groups in spectral differences.

A targeted PCA was conducted solely on PU and PU/Au samples to examine the nuanced

compositional variations between the two materials (**Figure 3a**). The PCA model demonstrated a cumulative explained variance of 100%, with the first principal component (PC1) accounting for 99.1% and the second principal component (PC2) accounting for 0.09%. The principal spectral characteristic affecting PC1 was located at 758 cm^{-1} with an eigenvalue of 0.578, whereas the band chiefly influenced PC2 at 1228 cm^{-1} (**Figure 3b**). The data indicate that vibrational modes related to out-of-plane C–H bending (758 cm^{-1}) are the primary differentiators between the original PU and the PU/Au nanocomposite. The C–N or C–O stretching at 1228 cm^{-1}, indicative of urethane connections, solely accounts for the discrepancies among the PU replicates. The presence of the 758 cm^{-1} bands, along with analogous vector bands at 946 cm^{-1} and 817 cm^{-1}, suggests that the introduction of gold nanoparticles subtly modifies the local chemical environment of particular functional groups within the polyurethane matrix, resulting in unique spectral signatures detectable through PCA. These bands demonstrated enhanced absorption in PU–Au, perhaps due to π-metal interactions or plasmonic field effects. Gold nanoparticles likely enhance conformational ordering (by plasmon-mediated intermolecular coupling) and dipole-dipole alignment, hence intensifying vibrational transitions in the aromatic domains [25].

These interactions are consistent with physical, rather than covalent, bonding between Au and the PU matrix. Previous studies involving carbon-based fillers (e.g., CNTs or graphene) have reported similar shifts due to electronic interactions, further supporting this interpretation [25]. Combining FTIR with chemometric methods, namely, PCA, it was feasible to discern small spectrum variations between PU, PU/Au, MDI, and polyol systems. The PCA model, together with a heatmap created by *MetaboAnalyst 6.0.0*, successfully displayed the distribution structures of the spectrum profiles, allowing a more complete knowledge of compositional changes and interaction dynamics [27].

To strengthen the FTIR analysis, FESEM was applied to investigate the surface characteristics of polyurethane (PU) and gold-modified PU (PU/Au) coatings (Figure 4a-d). Imaging acquired at magnifications of 200× to 5000× indicated smooth, continuous, and defect-free surfaces, even with greater Au concentrations. This suggests that gold inclusion did not degrade the film structure. The Au nanoparticles were uniformly dispersed with minimal aggregation, indicating high compatibility with the PU matrix, which was likely aided by the sonication-assisted casting method. Previous studies have found uniform AuNP distribution in polymer matrices [28].

Furthermore, to assess the thermal behavior of PU and gold-reinforced PU (PU/Au) composites, TGA and DSC were performed. These techniques provide complementary insights into thermal degradation patterns, phase transitions, and the influence of gold incorporation on polymer thermal stability. **Figure 5a** illustrates the derivative thermogravimetric (DTG) curves for PU, PU/Au, and Au samples. For pure PU, thermal decomposition initiates between 250 ℃ and 280 ℃, attributed to the evaporation of absorbed moisture and volatile oligomers. The primary degradation stage occurs between 320 ℃ and 400 ℃, corresponding to the breakdown of urethane linkages within the soft segment domains.

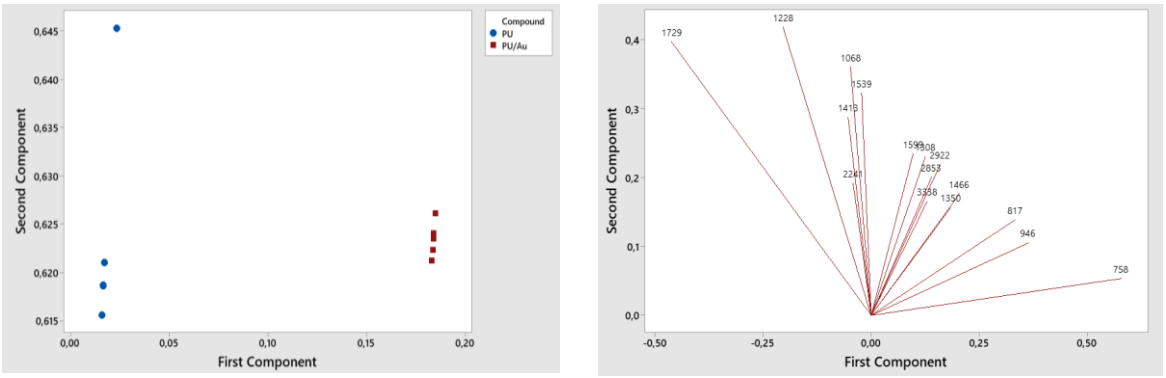

(a) **(b)**

Figure 3. Principal Component Analysis (PCA) of FTIR spectra of PU and PU/Au based on absorption at 16 selected wavenumbers: (a) Score plot showing sample distribution along PC1 and PC2; (b) Loading plot illustrating the contribution of each wavenumber to the principal components

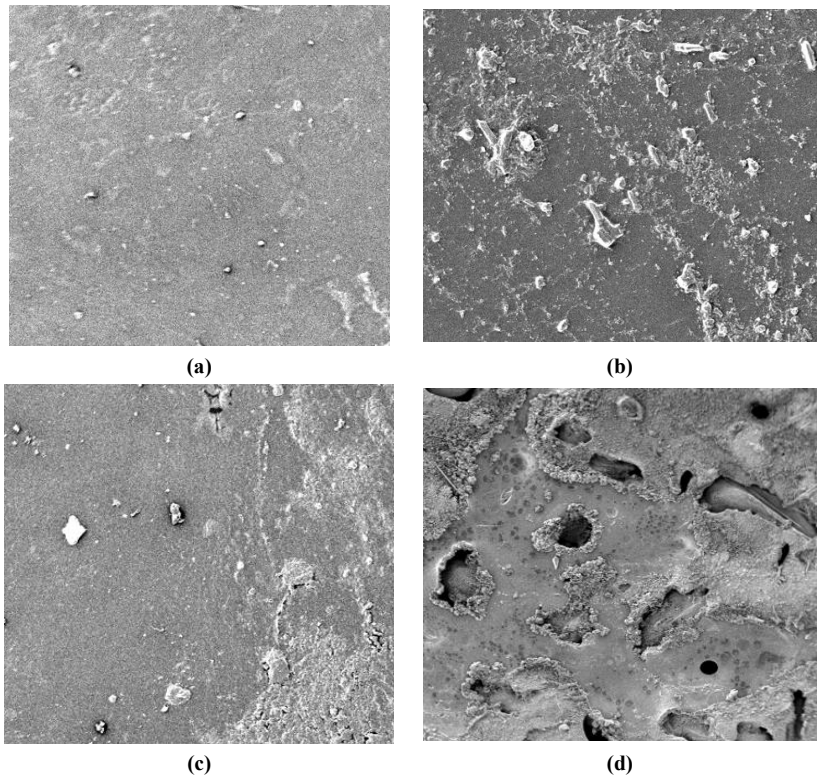

Figure 4. Surface morphology of PU and PU/Au (10%) captured via FESEM at 200× and 5000× magnifications (images a & b for PU; c & d for PU/Au).

This results in a substantial mass loss of approximately 40–50%. A subsequent degradation event, observed between 400 ℃ and 480 ℃ , is associated with the decomposition of hard segment structures derived from methylene diphenyl diisocyanate (MDI). By 500 ℃, over 90% of the PU mass is lost, leaving minimal residual char, indicating limited intrinsic thermal resistance. These results are consistent with previously reported thermal degradation behaviors of bio-based PUs [29]. In contrast, the gold sample demonstrates high thermal stability, with negligible mass loss below 600 ℃ and only a slight degradation (3–5%) in the range of 600–800 ℃, likely due to surface oxidation. The residual mass (~90%) confirms gold's excellent thermal endurance [30].

The PU/Au composites demonstrate enhanced thermal stability, as shown by the delayed onset of decomposition (210–240 ℃) and a slower, more gradual degradation phase between 290 ℃ and 400 ℃. The enhancement is most likely owing to gold's thermal shielding impact, which lowers polymer chain movement and heat transmission inside the matrix. The composite materials retain 10-20% of their mass even at 800 ℃, suggesting greater char formation and better thermal reinforcing. Previous research on gold-reinforced polymer systems supports the effectiveness of gold as a barrier and stabilizing agent [31,32].

TGA and derivative thermogravimetric (DTG) analyses were applied to study the thermal degradation behavior of PU and PU/Au composites by estimating degradation rates and weight loss. Nevertheless, these techniques do not properly record thermal transitions without considerable mass shift [33]. To address this limitation, DSC was utilized to find the glass transition temperature (*Tg*), pre-decomposition transitions, and phase mobility. A study by Luo et al. proposed a combination of TGA and DSC to achieve a satisfactory outcome on how Au affects the thermal behavior of the polymer composites [34]. **Figure 5b** demonstrates that the DSC curve for PU exhibits a thermal event between 30 ℃ and 60 ℃, indicating the evaporation of residual moisture and low molecular weight volatiles. Around 85 ℃, the polymer transitions from a rigid glassy state to a flexible rubbery phase. MDI-derived hard segments impact Tg behavior by increasing matrix stiffness. Minor endothermic drift above 100 ℃ could be due to internal chain rearrangements or instrument sensitivity to low-energy transitions [35].

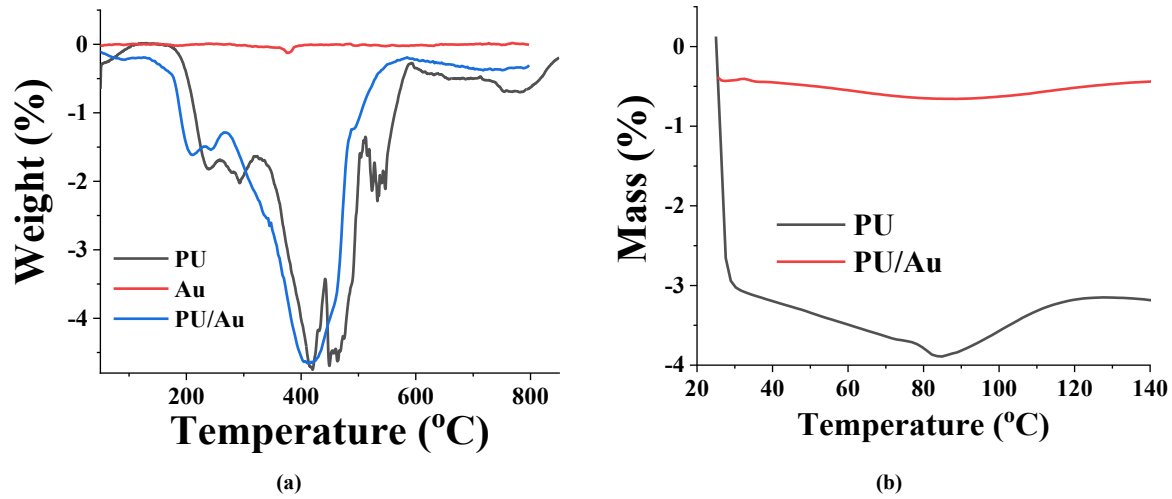

Figure 5. (a) DTG curves illustrating the thermal decomposition of PU, PU/Au (1%), and Au, and (b) DSC analysis of PU and PU/Au (1%)

On the other hand, the PU/Au composite has a more consistent DSC profile throughout the identical temperature range. The limited thermal activity, characterized by reduced baseline changes and the absence of substantial enthalpic events, indicates enhanced thermal stability and a more uniform matrix structure. Additionally, the very low moisture-related thermal response (less than 0.5% mass change) suggests enhanced barrier properties, likely resulting from the uniform dispersion of gold nanoparticles. This behavior aligns with findings from similar nanocomposite systems, where metal nanoparticles act as physical barriers that hinder moisture diffusion and molecular mobility [36]. The combined interpretation of TGA and DSC results confirms that Au incorporation contributes significantly to the thermal resilience of the PU matrix. Improvements in thermal transition stability, delayed degradation onset, and increased char residue collectively support the potential application of PU/Au composites in environments requiring enhanced thermal endurance, such as flexible electronics, thermal insulation, and protective coatings [37].

Furthermore, the PCA is applied to DTG data to extract the most discriminating thermal features between PU, PU/Au, and Au samples by reducing the dimensionality of temperature-resolved mass loss rates into principal components (**Figure 6a**). In this case, PC1 explains 91% of the total variance and captures the dominant difference between polymer-based samples (PU and PU/Au) versus Au, with the highest eigenvalue centered at 410 – 415 ℃ (eigenvalue of 0.145). This temperature region corresponds to significant degradation in PU and PU/Au, but not in Au, indicating that the nanoparticle sample remains thermally inert while the polymers decompose, thus driving separation along PC1. Meanwhile, PC2 accounts for 9% of the variance and shows its highest loading at 480 ℃ (eigenvalue of 0.193), which aligns with the primary degradation unique to PU (**Figure 6b**). PU/Au lacks a pronounced thermal event at this temperature, suggesting that the incorporation of Au nanoparticles suppresses or modifies this primary degradation phase.

A focused PCA was performed just on PU and PU/Au samples to investigate the slight degradation differences between the two materials (**Figure 6c**). PCA conducted on the DTG profiles of PU and PU/Au samples demonstrated that the first principal component (PC1) encompasses 100% of the variation, signifying that the principal origin of thermal differentiation is exclusively aligned with this axis. The maximum PC1 loading (eigenvalue of 0.203) is observed at 480 ℃, with secondary loadings at 533–535 ℃ (eigenvalues of 0.152–0.146) (**Figure 6d**). Both temperature ranges relate to the first and terminal degradation phases of polyurethane, generally linked to the breakdown of thermally stable hard segments. PCA elucidates the major alterations in thermal behavior and demonstrates how gold nanofillers modify the thermal decomposition pathway of polyurethane, influencing both the intensity and sequencing of degradation events.

To evaluate the electrochemical performance and conductivity enhancements of the developed composites, Electrochemical Impedance Spectroscopy (EIS) was conducted on pristine polyurethane (PU) and PU/Au films containing varying concentrations of gold nanoparticles (1, 2, 5, and 10 wt%). Measurements were performed in phosphate-buffered saline (PBS, 0.01 mol•L^{-1}, pH 7.2) to simulate physiological conditions, and data were processed using *ZView software* by fitting the

impedance spectra to a Randles equivalent circuit. This model was chosen due to its well-established relevance in describing charge-transfer and ion-diffusion behavior at electrode/electrolyte interfaces [38].

As illustrated in **Figure 7**, all samples exhibit canonical EIS features: a semicircular arc in the high-frequency region corresponding to charge transfer resistance (*Rct*), followed by a linear tail at lower frequencies indicative of Warburg diffusion. This response confirms that the system follows a mixed kinetic-diffusion-controlled mechanism typical of electroactive coatings. The Nyquist plot for the pure PU sample shows a large semicircle diameter, reflecting its intrinsically insulating nature and high bulk resistance (*Rb*). With increasing Au content, a progressive decrease in semicircle diameter is observed, indicating a systematic reduction in *Rb*. This trend can be attributed to the formation of conductive pathways facilitated by homogeneously distributed gold nanoparticles within the PU matrix. At higher concentrations (especially 5 and 10 wt%), the Au level is sufficient to exceed the electrical percolation threshold, allowing for more efficient electron transport across the polymer composite. Identical resistance and impedance have been reduced due to nanoparticle-induced conductive networks that have been seen in metal-filled polymer systems [39,40].

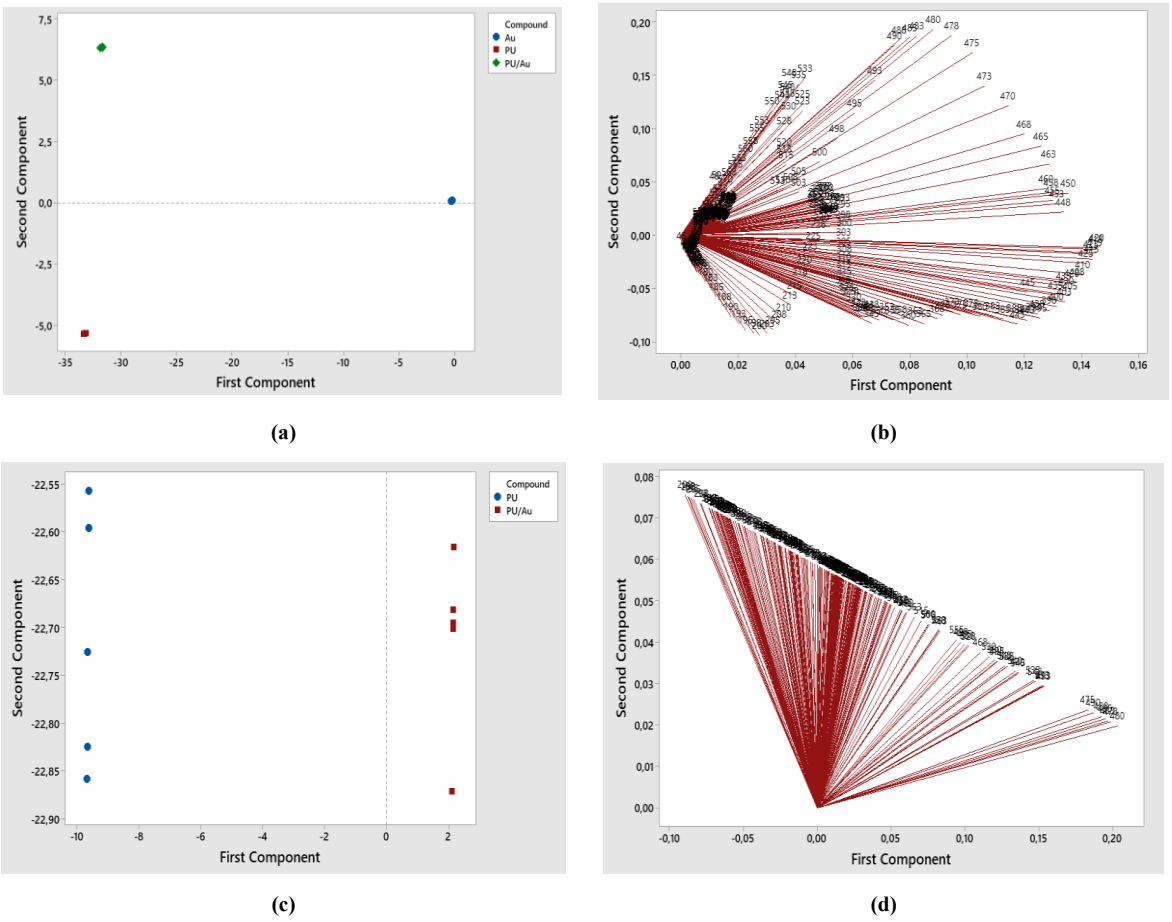

Figure 6. PCA of DTG data of PU, PU/Au, and Au; Score plot (a) showing sample distribution along PC1 and PC2; Loading plot (b) illustrating the contribution of each degree to the principal components. PCA of DTG data of PU and PU/Au; Score plot (c) showing sample distribution along PC1 and PC2; Loading plot (d) illustrating the contribution of each degree to the principal components

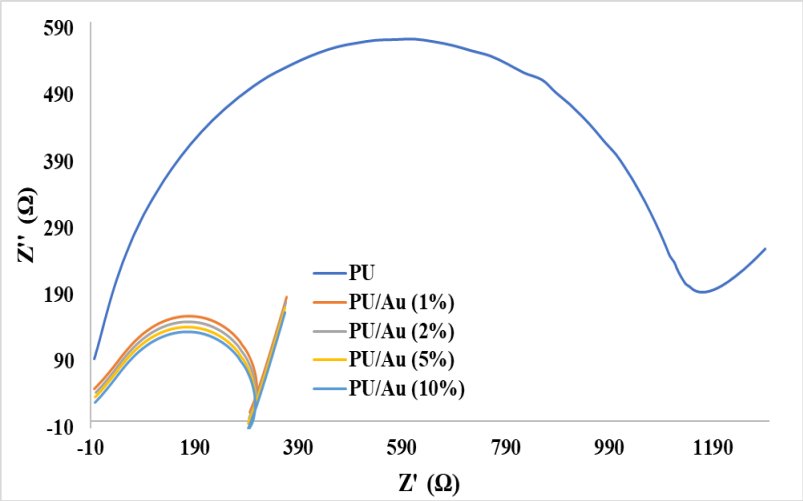

Figure 7. Electrochemical impedance profiles of PU and PU/Au coatings with different Au loadings

The Randles circuit was applied to acquire quantitative insights and establish a clear relationship between Rb values and Au concentration, demonstrating the multifaceted role of Au nanoparticles. In addition to enhancing mechanical strength and thermal stability, Au significantly improves the electrochemical activity of the otherwise insulating PU matrix. Compared to other conventional fillers, the combination of Au and AC provides synergistic benefits: AC contributes high surface area and electrical conductivity, while Au nanoparticles enhance charge transfer, thermal stability, and catalytic activity. This dual functionality leads to superior performance in thermal, structural, and electrochemical properties compared to PU composites with single fillers such as AC alone or other metal nanoparticles. As a result, PU/Au-AC composites are particularly promising for applications such as flexible electronics, biosensors, corrosion-resistant coatings, and bioelectronic devices that require a balance of conductivity, durability, and environmental compatibility [41,42]. Furthermore, this development aligns with UN Sustainable Development Goals, particularly SDG 9 (Industry, Innovation, and Infrastructure) and SDG 12 (Responsible Consumption and Production), by promoting innovative high-performance materials that deliver societal and environmental benefits through more efficient energy storage, sensing, and catalytic systems. Collectively, these advantages underscore the potential of Au-AC/PU composites as environmentally responsible and technologically advanced solutions.

Conclusion

This work demonstrates how satisfactory the Au is combined with a bio-based PU that greatly enhances its structural, thermal, and electrochemical characteristics by identifying using FTIR, TGA, DSC, FESEM, and EIS. A chemometric approach coupled with the FTIR and TGA revealed subtle molecular interactions and improvement in the thermal stability, while FESEM confirmed uniform gold dispersion. Thermal investigations revealed delayed degradation and increased char output, while EIS indicated lower bulk resistance due to the addition of the Au. These findings could potentially be considered the PU/Au composites for advanced applications, including flexible electronics, sensing, and coatings.

Acknowledgement

The authors would like to acknowledge and express their gratitude to Universiti Malaysia Sarawak (UNIMAS) via the International Matching Grant (INT/F07/UNS/86787/2025). The authors also gratefully acknowledge the Royal Society of Chemistry for the Researcher Development and Travel Grant (D25-3501826908). Appreciation is also extended to the Faculty of Resource Science & Technology (FRST) for providing essential research facilities and technical support.

References

1. Wan, W., Deng, P., Guo, H., Zhou, Y., Zhang, H., and Zhou, X. (2025). A novel approach to conductive self-healing composites: Incorporating nickel-plated carbon fibers into layered polyurethane urea. *Materials Today Communications*, 42, 111237.
2. Partanen, K., Lee, D. S., Omoboye, A., McEleney, K., Chen, R. X. Y., and She, Z. (2023). Improvement of low-cost commercial carbon screen-printed electrodes conductivities with controlled gold reduction towards thiol modification. *Journal of the Electrochemical Society*, 170, 092510.

3. Weber, C. J., Strom, N. E., Simoska, O. (2024). Electrochemical deposition of gold nanoparticles on carbon ultramicroelectrode arrays. *Nanoscale*, 16, 16204-16217.
4. Graziano, F., Tortora, C., Vespini, V., Rippa, M., Grilli, S., Marani, R., Coppola, S., Stella, E., Ferraro, P. (2023). Multimodal non-destructive techniques for composite inspection. *Proceedings of SPIE - The International Society for Optical Engineering*, 126210s.
5. Chen, Q., Zhao, C., Fang, Y., Zhang, R., Song, N., Ding, P., Han, Y. (2025). The Prediction of Tensile Strength Performance of Fiber-Reinforced Composites Based on a Knowledge Graph Constructed From Material Literature. *Polymer Composites*, 46, 14404-14421.
6. Li, T., Zhang, S. X., Huang, H. H., Chen, W. M. (2022). The machine learning method for overlapping peak decompositions in differential scanning calorimetry. *Thermochimica Acta*, 708, 179123.
7. Wesolowski, M., Leyk, E. (2023). Coupled and Simultaneous Thermal Analysis Techniques in the Study of Pharmaceuticals. *Pharmaceutics*, 15, 1596.
8. Angin, N., Ertas, M., Caylak, S., Fidan, M.S. (2023). Thermal and electrical behaviors of activated carbon-filled PLA/PP hybrid biocomposites. *Sustainable Materials and Technologies*, 37, e00655.
9. Singh, M., Sarkar, A. (2018). Comparative study of the PLSR and PCR methods in laser-induced breakdown spectroscopic analysis. *Journal of Applied Spectroscopy*, 85, 5, 962-970.
10. Carnoli, A., oude Lohuis, P., Buydens, L.M.C., Jansen, J.J., Tinnevelt, G.H. (2024). Applications of Rasch modeling in chemometrics: Binary data analysis and analytical platform selection. *Chemometrics and Intelligent Laboratory Systems*, 245, 105045.
11. Munir, M. A., Jamal, J. A., Said, M. M., Ibrahim, S., Ahmad, M. S. (2023). Polyurethane application to transform screen-printed electrode for rapid identification of histamine isolated from fish. *Scientifica*, 2023, 1, 5444256.
12. Naseem, K., Abrar, E., Haider, S., Alam, K. (2024). Polyurethane-based nanocomposite for catalytic reduction of toxic dyes. *Polymers for Advanced Technologies*, 35, 4, e6372.
13. Rojek, B., Wesolowski, M. (2017). Compatibility studies of hydrocortisone with excipients using thermogravimetric analysis supported by multivariate statistical analysis. *Journal of Thermal Analysis and Calorimetry*, 127, 543-553.
14. Beattie, J. R., Esmonde-White, F. W. L. (2021). Exploration of principal component analysis: Deriving principal component analysis visually using spectra. *Applied Spectroscopy*, 75, 361-375.
15. Munir, M.A., Inayatullah, A. (2024). The chemometric approach for verification of paracetamol level in pharmacies products using spectrophotometer UV-Vis. *ASM Science Journal*, 19, 1-15.
16. Wang, X., Yu, T., Wu, Y., Shen, Y., Wang, Y., Hang, Y. (2023). Study on mechanical properties of two-component polyurethane based on multi-scale molecular simulation. *Materials*, 16, 1006.
17. Eren, B., Karacoban, E. D., Erdogan, B. (2025). Synthesis and characterization of UV-curable polyurethane acrylates derived from trimethylolpropane and hydroxyethyl methacrylate: Effect of 2-hydroxyethyl methacrylate (HEMA) content on thermal stability, gloss properties, and microstructure. *Polymer Engineering and Science*, 65, 327-337.
18. Liu, Z., Ma, Y. (2025). Recyclable dynamic covalent networks derived from isocyanate chemistry: The critical role of electronic and steric effects in reversibility. *ChemSusChem*, 2500436.
19. Hennig, K., Vacun, G., Thude, S., Meyer, W. (2025). Photocurable Crosslinker from Bio-Based Non-Isocyanate Poly(hydroxyurethane) for Biocompatible Hydrogels. *Polymers*, 17, 1285.
20. Avdeliodi, E., Tsioli, A., Bokias, G., Kallitsis, J. K. (2024). Controlling the synthesis of polyurea microcapsules and the encapsulation of active diisocyanate compounds. *Polymers*, 16, 270.
21. Ravishankar, K., Muthusamy, S., Durai, S. K., Murugan, G., Koushik, A. V. V., Thirumal, N., Bhaskar, S. N., Jaisankar, S. N. (2024). Microwave-assisted carbamation and one-pot phosphorylation-carbamation of starch using molten urea as a reactive solvent. *ACS Sustainable Resource Management*, 1, 2203-2213.
22. Silipigni, L., Cutroneo, M., Torrisi, A., Torrisi, L. (2023). Modifications of the optical and vibrational properties in polylactic acid films by the addition of gold nanoparticles produced by laser ablation in chloroform. *Radiation Effects and Defects in Solids*, 178, 182-193.
23. Manzoli, M., Chiorino, A., Vindigni, F., Boccuzzi, F. (2012). Hydrogen interaction with gold nanoparticles and clusters supported on different oxides: A FTIR study. *Catalysis Today*, 181, 62-67.
24. Martis, L. J., Parushuram, N., Sangappa, Y. (2021). Structural, morphological and electrical properties of PVA/Au nanocomposite films. *Materials Today: Proceedings*, 49, 1680-1683.
25. Yi, J., You, E. M., Ding, S. Y., Tian, Z. Q. (2020). Unveiling the molecule–plasmon interactions in surface-enhanced infrared absorption spectroscopy. *National Science Review*, 7, 1228-1238.
26. Pandey, A. K., Pal, T., Sharma, R., Kar, K. K.

(2020). Study of matrix–filler interaction through correlations between structural and viscoelastic properties of carbon-filler/polymer-matrix composites. *Journal of Applied Polymer Science*, 137, 48660.

27. Shukla, U. (2025). Fourier transform infrared spectroscopy: A power full method for creating fingerprint of molecules of nanomaterials. *Journal of Molecular Structure*, 1322, 140454.
28. Sharifzadeh, E., Karami, M., Ader, F. (2023). Formation of nanoparticle aggregates and agglomerates in polymer nanocomposites and their distinct impacts on the mechanical properties. *Polymer Engineering and Science*, 63, 1303-1313.
29. Lei, X., Ou, Y., Wang, Y., Ma, J., Lin, Q. (2024). Thermal decomposition behavior of polylactic acid-based polyurethane resin. *Polish Journal of Environmental Studies*, 33, 1225-1236.
30. Mahadik, S. A., Thakur, S., Fernando, P. D. (2024). Designing polyaniline films with tailored thermal, optical, and hydrophobic properties via gold nanoparticle integration. *Journal of Industrial and Engineering Chemistry*, 130, 382-391.
31. Murtaza, A., Uroos, M., Sultan, M., Muazzam, R., Naz, S. (2021). Enhancing catalytic potential of gold nanoparticles by linear and cross-linked polyurethane blending. *RSC Advances*, 11, 26635-26643.
32. Gul, M., Kashif, M., Muhammad, S., Azizi, S., Sun, H. (2025). Various methods of synthesis and applications of gold-based nanomaterials: A detailed review. *Crystal Growth & Design*, 25, 7, 2227-2266.
33. Ornaghi, H. L., Nohales, A., Asensio, M., Gomez, C. M., Bianchi, O. (2024). Effect of chain extenders on the thermal and thermodegradation behavior of carbonatodiol thermoplastic polyurethane. *Polymer Bulletin*, 81, 2267-2286.
34. Luo, Y., Pu, K., Gao, J., Zhou, Y., Wan, J., Bai, X. (2024). Thermal degradation behavior and kinetics of porous polymer based on high functionality components. *Journal of Applied Polymer Science*, 141, e55304.
35. Kumagai, S., Motokucho, S., Yabuki, R., Anzai, A., Kameda, T., Watanabe, A., Nakatani, H., Yoshioka, T. (2017). Effects of hard- and soft-segment composition on pyrolysis characteristics of MDI, BD, and PTMG-based polyurethane elastomers. *Journal of Analytical and Applied Pyrolysis*, 126, 337-345.
36. Joraid, A. A., Al-Maghrabi, M. A., Alshehry, A. A. (2025). Effect of SiO_2 nanoparticles on the melt-crystallization kinetics and mechanical behavior of polypropylene. *Journal of Polymer Research*, 32, 196.
37. Luo, Y., Liu, L., Chen, X., Chen, X., Chen, J., Li, Y., Zhu, Y. (2025). Enhancing thermal conductivity and joule heating performance in flexible TPU-based composites through optimized interfacial connectivity of hybrid fillers. *Composites Communications*, 55, 102297.
38. Patel, B., Sorrentino, A., Vidakovic-Koch, T. (2025). Data-driven analysis of electrochemical impedance spectroscopy using the Loewner framework. *iScience*, 28, 111987.
39. Sun, B., Li, G., Wu, Y., Gai, J., Zhu, M., Ji, W., Wang, X., Zhang, F., Li, W., Hu, J., Lou, Y., Feng, G., Han, X., Dong, J., Peng, J., Pei, J., Wan, Y., Li, Y., Ma, L. (2024). Ce-MOF@Au-Based Electrochemical immunosensor for apolipoprotein A1 detection using nanobody technology. *ACS Applied Materials & Interfaces*, 16, 58405-58416.
40. Guo, Y., Li, C., Guo, W., Zhang, X., Wang, L., Zhang, W., Zou X., Sun, Z. (2024). Advanced electrochemical biosensing toward staphylococcus aureus based on the RPA-CRISPR/Cas12a system and conductive nanocomposite. *Journal of Agricultural and Food Chemistry*, 72, 22918-22925.
41. Munir, M. A., Rahmawati, F., Jamal, J. A., Rahmawati, E., Fajriyaningsih, F. Z., Putri, F. R., Gunawan, A. (2024). Fabrication and characterization of new bio-based electrode polyurethane: diverse conducting materials impacts such as graphene oxide, gold, and carbon nanotube. *Green Chemistry Letters and Reviews*, 17, 2355235.
42. Omidiyan, M., Srinoi, P., Pooria, T., Lee, T. R. (2024). Review of light-activated antimicrobial nanoparticle-polymer composites for biomedical devices, *ACS Applied Nano Materials*, 7, 8377-8391.